

## THE SETTLING OF SUSPENSIONS PROMOTED BY RIGID BUOYANT PARTICLES

YIANNIS P. FESSAS and RALPH H. WEILAND†

Department of Chemical Engineering, Clarkson University, Potsdam, NY 13676, U.S.A.

(Received 30 March 1983; in revised form 10 December 1983)

**Abstract**—When substantial numbers of buoyant particles are mixed with a sedimenting suspension of heavy particles, the two types of solids undergo rapid lateral segregation from each other. Streams 3–5 mm in diameter containing the less populous species form and flow through a concentrated continuum suspension of the more populous species. This buoyancy driven convection results in greatly enhanced sedimentation rates. A theory is developed on the premise that streams move in plug flow with all resistance to motion confined to a thin lubricating layer at the stream-continuum interface. The model is compared with experimental data and is shown to account correctly for the effect of each system parameter on the observed settling rates.

### INTRODUCTION

The separation of suspended solids from a liquid is a common processing step applied on a huge scale in the chemical, mining and metallurgical industries, as well as in environmental control operations. Gravity, which is relatively ineffective when the particles are small or have a density only slightly greater than the fluid, is the usual driving force. As a result, settling vessels of very large diameter are required. Although the concomitantly large fluid holdup can be used to advantage in dampening process fluctuations, maintaining a large inventory can be costly if the fluid is a valuable one. Any practical means of accelerating sedimentation rates would be beneficial in reducing the size of new separations equipment and improving the handling capacity of existing vessels.

Flocculation is the most widely practiced method for enhancing gravity settling rates. Flocculants, which are usually polyelectrolytes, are subject to shear degradation, are fairly expensive, and cannot be recovered. Sedimentation rates have also been found to be increased by the presence of inclined surfaces and stacks of inclined plates are now found in so-called lamella settlers. Inclined plates allow the formation of clear fluid beneath them so that, in effect, they provide an enormous surface area for particle deposition yet they present only a small depth of fluid through which the settling particles must fall. Their advantages are counterbalanced somewhat, however, by the fact that they are difficult to feed uniformly and that the downflow of suspension along the surface of the plates is subject to a shear instability (resulting from the upflow of overlying fluid) which tends to resuspend particles into the clear fluid and so limits capacity.

In 1979, Weiland and McPherson reported the first results of an entirely new technique for improving sedimentation rates. By adding a second buoyant particulate phase to a normal suspension settling under gravity, they found that sedimentation rates could be increased by several fold. The presence of the buoyant particles resulted in a rapid *lateral* separation of the two species of particles into large-scale convection currents or streams. These streams were gravity driven to flow in the vertical direction so that in addition to the normal settling velocity of a particle in a fluid, a large convective component was superimposed. The convective component was found to be so large that settling rates could be increased by factors of five or ten. These streams of suspension were found to contain exclusively one species of particle or the other (Fessas & Weiland 1981, 1982). Consequently, the suspensions that collected at each end of the settling vessel were pure components.

†Author to whom correspondence should be addressed.

The process can be more easily understood when it is realized that three-phase settling progresses through a number of stages. Soon after the initially well-mixed suspension (figure 1a) begins to settle, a suspension containing only buoyant solids forms over the three-phase region while a suspension containing only heavy solids forms beneath it (figure 1b). At the extreme top and bottom of the vessel, beds of buoyant and heavy solids are deposited. The three-phase region is the one in which convection predominates and which is responsible for the enormously increased settling rates. Gradually, the three-phase region shrinks until, at disengagement, the interfaces separating the buoyant suspension from the three-phase region, and the three-phase region from the heavy suspension pass through each other (figure 1c). Following this, we are left with a rising buoyant suspension, a settling heavy suspension and a clear fluid layer which continues to expand between the two (figure 1d). The entire sedimentation process ends (figure 1e) when all particles are fully deposited as sediments at the top and bottom of the settling vessel.

Although a small amount of preliminary data has been reported elsewhere (Fessas & Weiland 1981, 1982), the results of the first comprehensive investigation of this new and exciting phenomenon are reported in the present communication; we deal with the settling of *model* suspensions in the presence of buoyant particles. The solids used are nonfloculating, approximately-spherical particles of controlled size. Flocculants were not used for two reasons. First, one can view buoyant particles as an inexpensive recycleable substitute for flocculants and, second, we wish to examine the use of buoyant particles in isolation from other methods for enhancing settling rates.

The experimental data have been correlated using a simple model of the steady streaming process. This model assumes that the streaming suspension is in plug flow and that viscous shear effects are confined to a thin lubricating layer at the surface of the streams. For convenience, the model and general correlation are presented first. The effect of each system parameter on the settling velocity and on the concentrations of the resulting separated suspensions are then treated in turn.

#### A THEORY OF THREE-PHASE SEDIMENTATION

The qualitative observations of three-phase sedimentation described by Fessas & Weiland (1981) indicate that over a wide range of conditions of suspension concentration,

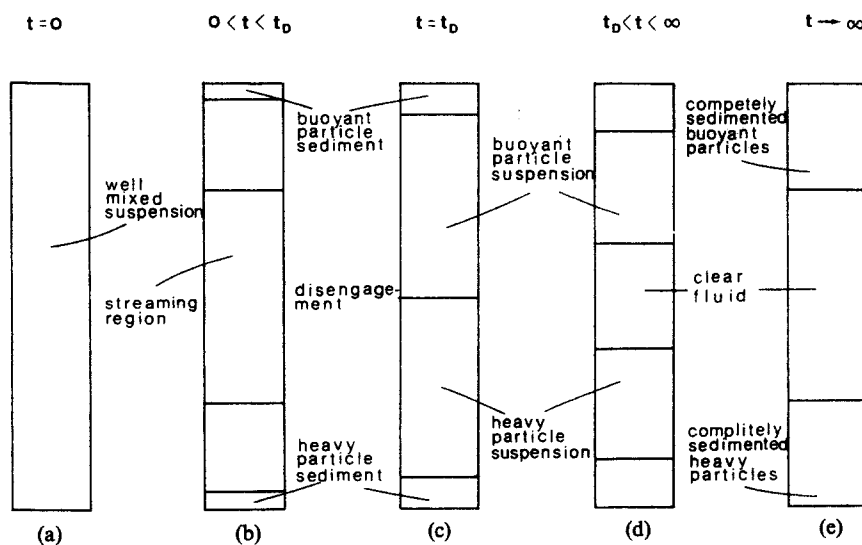


Figure 1. Schematic of the various stages occurring during three-phase sedimentation; (a) well-mixed suspension, (b) the three-phase streaming period, (c) disengagement, (d) independently settling buoyant and heavy suspensions, (e) packed beds.

particle size and density, and so on, the particulate species present in the smallest volumetric amount flows through the suspension in the form of streams or convection currents. On the other hand, particles of the species in the greater volumetric concentration segregate, not into fingers, but into a more concentrated continuum suspension in which the streams of the other species are embedded. Thus, in three-dimensional three-phase settling (e.g. in a tube) the two types of particles separate from each other laterally; the initially uniform three-phase mixture evolves quickly into streams of the less populous species flowing through a continuum of the more populous one. Ultimately a steady state is achieved—particle velocities in both the streams and the continuum become constant, although the lengths of the streams shrink as sedimentation proceeds. Because the induction period in which the fingering motion is set up is very short relative to the total separation time, such a steady state model will account for events during most of the accelerated rate (three-phase) period.

Because the streams form from an initially uniform three-phase mixture, part of the fluid in this mixture finds its way into the streams while the rest remains behind in the segregated continuum. It will be assumed that the way in which fluid apportions itself between streams and continuum depends on the initial volumetric proportions of the two types of particles. The result will be a model that predicts the concentrations of the suspensions that appear at either end of the sedimentation vessel. These concentrations are then used to calculate the densities of streams and continuum, hence, the driving force for the flow, and the composition of the thin lubricating layer between streams and continuum; the latter is needed to estimate the viscosity of the mixture in the layer.

#### *Particle concentrations and fluid apportioning*

A typical horizontal cross-section through a well-mixed suspension of heavy and buoyant particles of diameters  $d_H$  and  $d_L$ , respectively, is shown in figure 2(a). Following lateral segregation, the same cross-section might look like figure 2(b). Streams, of course, are actually particle-fluid mixtures; thus, part of the fluid content of the initial suspension can be identified as belonging to streams while the remainder is identified with the continuum suspension of the other type of particles. Such a notion of fluid apportioning is not new; for example, Bradley (1965) and Bhatti *et al.* (1980) have noted that fluid is,

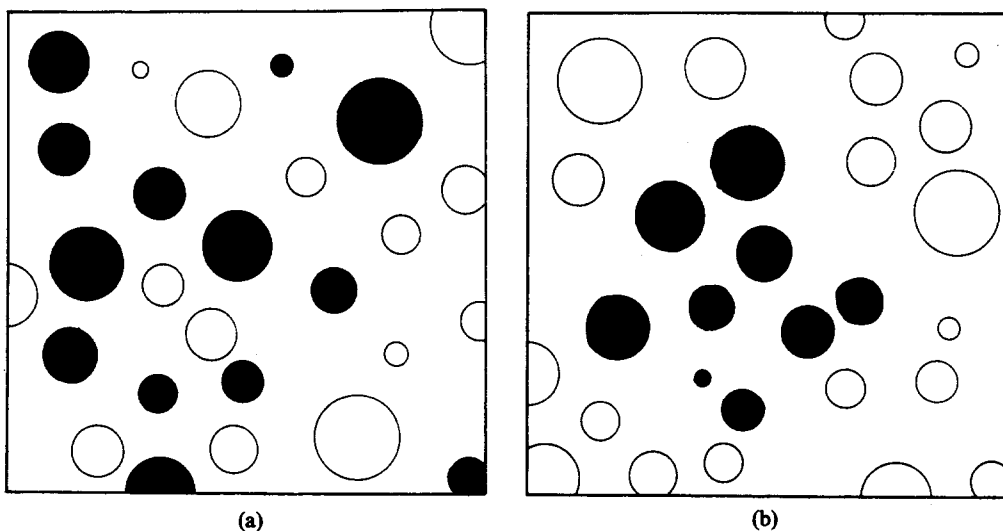


Figure 2. Typical horizontal cross-section through a three-phase suspension (a) when it is well mixed and (b) following lateral segregation.

in some sense, trapped with particles in clusters. Crabtree & Bridgewater (1969), Chesters *et al.* (1980), Rietema & Ottengraf (1970) and Hussain & Siegel (1976) have all suggested similar fluid entrapment with gas bubbles and bubble plumes.

Consider first the initial, well-mixed suspension. If  $\epsilon$  is the fluid volume fraction, then clearly

$$C_H + C_L + \epsilon = 1 \quad [1]$$

where  $C_L$  and  $C_H$  represent the volume fractions of heavy and light particles, respectively. Upon lateral segregation, the fluid splits into fractions  $f_H$  and  $f_L$  associated with the respective kinds of particles:

$$f_H + f_L = \epsilon \quad [2]$$

and we can define new particle concentrations  $C_H^*$  and  $C_L^*$  within segregated regions as

$$C_H^* = C_H / (C_H + f_H) \quad [3]$$

$$C_L^* = C_L / (C_L + f_L). \quad [4]$$

Rearrangement leads to

$$C_H / C_H^* + C_L / C_L^* = 1 \quad [5]$$

which is just the expression of a volume balance. Equation [5] is remarkably similar to one derived by Smith (1965) for the differential sedimentation of two particulate species both of density greater than the suspending fluid:

$$C_1 / K_1 + C_2 / K_2 = 1 \quad [6]$$

in which  $C_1$  and  $C_2$  are superficial concentrations and  $K_1$  and  $K_2$  are effective concentrations within cells (of the original cell model of Happel 1958). It is interesting to note that even if  $K_1$  and  $K_2$  could have been measured (which they could not) Smith was forced to restrict his attention to systems of heavy particles only, because the force balances he used to relate these  $K$ -values to species densities and concentrations resulted in a negative value of  $K$  for a buoyant species.

We now need to postulate how the fluid distributes itself between the streams and the continuum. Unfortunately there is no deductive way to do this; however, suppose that each solid species entrains fluid in direct proportion to its initial volumetric concentration in the original suspension. Such a postulate might be adequate for spherical particles; however, if the particles are of irregular shape (as some of the particles used in the present study were), it is likely that these would entrain more fluid than spherical ones. A measure of shape that seems especially appropriate to account for the additional entrainment is the void fraction of unconsolidated packed beds of these particles. Denoting the latter by  $\epsilon_H^\infty$  and  $\epsilon_L^\infty$ , we must have that  $f_H \propto \epsilon_H^\infty C_H$  and  $f_L \propto \epsilon_L^\infty C_L$ . Assuming the constant of proportionality to be the same in both cases, it can be determined from [2] with the result that fluid is distributed according to

$$f_H = \frac{\epsilon_H^\infty C_H \epsilon}{\epsilon_H^\infty C_H + \epsilon_L^\infty C_L}; \quad f_L = \frac{\epsilon_L^\infty C_L \epsilon}{\epsilon_H^\infty C_H + \epsilon_L^\infty C_L}. \quad [7]$$

When these expressions are used in [3] and [4], we obtain the following expressions for the volume concentrations of the stream and continuum suspensions:

$$C_H^* = \frac{\lambda C_H + C_L}{\lambda + C_L(1 - \lambda)}; \quad C_L^* = \frac{\lambda C_H + C_L}{1 - C_H(1 - \lambda)} \quad [8]$$

where

$$\lambda = \epsilon_H^\infty / \epsilon_L^\infty. \quad [9]$$

When [8] and [9] are combined with [5] we obtain

$$\frac{1}{C_H^*} = \lambda \frac{1}{C_L^*} + (1 - \lambda). \quad [10]$$

This is a particularly useful form of [5]. Not only does it allow us to check the consistency of experimental data by the closure of a volume balance; it also allows us to evaluate the efficacy of our postulates about fluid apportioning. Of course, experimentally we cannot measure concentrations in the streams and continuum directly but we can certainly measure concentrations of the suspensions formed after vertical disengagement of the buoyant and heavy particles from each other. Thus, [10] can be used also to check the validity of any assumption about the concentrations in streams and continuum being the same as those of the separated suspensions. Finally, if the experimental evidence validates [10], we have a means of predicting  $C_H^*$  and  $C_L^*$  from a knowledge of initial concentrations and packed bed voidages.

#### *Settling and rise velocities*

In three-phase sedimentation, a stream is a mixture of particles of one density in a suspending fluid which flows vertically upward or downward through a surrounding mixture composed of fluid, and particles of another density. Because the particles in both the stream and the continuum mixture are of a density different from the fluid, particles are always in a state of motion relative to the fluid enveloping them. Thus, particles of both types (i.e. densities) exhibit the usual sort of sedimentation relative to the fluid. In addition, however, because the bulk density of the streaming suspension differs from that of the continuum suspension, gravity drives a convective flow of streams relative to continuum.

Consider an isolated stream of fluid and particles of one density, embedded in a continuum suspension of fluid and particles of another density. The stream has diameter  $D$  and contains a volume fraction  $C_s$  of solids, while the surrounding suspension contains a solids fraction  $C_c$ . At this point, whether the stream contains the heavy or the light particles is immaterial; what is important is that the stream contains particles of exclusively one density or other, while the continuum contains particles of only the opposite kind.

We take conventional laboratory coordinates fixed in the walls of the sedimentation vessel. In these coordinates, the particle velocity derives from two components; one component is convective,  $U_c$ , and results from the flow of the stream. The other component,  $U_p^*$ , is a hindered settling velocity arising from the fact that within the stream itself, particles are moving relative to the surrounding fluid because their density differs from that of the fluid. Thus, the measured particle velocity is

$$U_p = U_p^* + U_c. \quad [11]$$

The contained fluid also has a velocity,  $U_f$ , given by

$$U_f = U_b + U_c \quad [12]$$

in which  $U_b$  is the return fluid flow produced during normal hindered settling and resulting from the sedimenting (upward or downward) particles displacing fluid. This return flow is given by

$$U_b = -U_p^* C_p / (1 - C_p) \quad [13]$$

where  $C_p$  is the volume fraction of particles in the suspension.

The velocity of the stream is obtained by dividing the total local volume flux by the total local volume concentration of material in the stream. Thus,

$$U'_s = \frac{U_p C_p + U_f (1 - C_p)}{C_p + (1 - C_p)} \quad [14]$$

A little algebra shows that this is just

$$U'_s = U_p - U_p^* \quad [15]$$

and we note that  $U'_s$  is the velocity of a stream relative to fixed coordinates. The same expression holds for the continuum suspension but with the subscript  $s$  replaced by  $c$ .

The velocity of fluid mechanical interest is that of the stream relative to the continuum suspension. Since  $U'_s$  and  $U'_c$  are in opposite directions, the relative velocity is just

$$U_{\text{rel}} = U'_s + U'_c \quad [16]$$

The experimentally-measured quantities are the velocity of a particle in a stream ( $U_{ps}$ ), in the continuum ( $U_{pc}$ ) and their corresponding hindered settling velocities at stream and continuum concentrations ( $U_{ps}^*$  and  $U_{pc}^*$ ); in these terms, [16] is

$$U_{\text{rel}} = U_{ps} - U_{ps}^* + U_{pc} - U_{pc}^* \quad [17]$$

where the subscripts  $ps$  and  $pc$  refer to particles in the stream and continuum, respectively.

The buoyancy force that drives the flow depends on the density difference between the streaming suspension and the continuum:

$$\Delta\rho_s = C_s(\rho_{ps} - \rho_f) + C_c(\rho_f - \rho_{pc}) \quad [18]$$

where  $ps$  and  $pc$  have the meaning given above.

Under conditions of steady flow, gravitational and viscous forces balance. Visual observations of particle motion within streams in a two-dimensional geometry leads us to postulate that viscous shear is confined to a thin layer at the interface between the stream and the continuum through which it flows; otherwise, both stream and continuum are taken to be in plug flow. Having proposed the existence of a shear layer, we need to make further postulates about (i) its thickness, (ii) its composition and (iii) a constitutive relation for the material filling it.

Certain anomalies in the viscosity of suspensions measured in capillary tubes by Maude & Whitmore (1956) have been explained by the existence of a particle-free lubrication or plasmatic layer near the wall of the tube. This layer has been photographed by Karnis *et*

*al.* (1966) and its width has been found to be a function of particle size, independent of capillary diameter. In the present case of streaming through a continuum of suspension, we propose that the shear layer thickness,  $\delta$ , is a linear function of the sum of the particle diameters. Thus, if the particles in the stream and the continuum have diameters  $d_s$  and  $d_c$ , respectively, then

$$\delta = k'(d_s + d_c) \quad [19]$$

in which the constant of proportionality is taken to be independent of the concentrations of the individual types of particles although it may depend on total concentration.

The shear layer is almost certainly not filled with particle-free fluid. We will postulate that the concentration of each particle species in this layer is proportional to its concentration in the bulk segregated region (stream or continuum) and that it is also dependent on particle size. This is the simplest mixing rule we can think of and it derives from the first postulate that gap thickness depends on  $(d_s + d_c)$ . Thus, for the streaming and continuum species, respectively,

$$C_{sg} = d_s C_s / (d_c + d_s); \quad C_{cg} = d_c C_c / (d_c + d_s) \quad [20]$$

in which subscripts *sg* and *cg* refer to the streaming and continuum species in the gap, respectively. The total concentration of particles in the lubrication layer is then

$$C_g = (d_s C_s + d_c C_c) / (d_c + d_s) \quad [21]$$

since  $C_{sg}$  and  $C_{cg}$  are themselves volume fractions.

The third item to be addressed, namely a constitutive relation for the gap material, is less straightforward. Because the flow appears to be a creeping one in which shear rates are low, we will assume that the mixed suspension in the gap behaves as a Newtonian fluid. However, estimates of the relative viscosity of bimodal (in size) dispersions are not easily obtained. Indeed, whether the relative viscosity of monodisperse suspensions is independent of particle size has been an issue for many years, largely as a result of capillary viscometers being used for measurement. However, Chong *et al.* (1971) constructed a special orifice viscometer which eliminated the particle-free lubrication layer characteristic of capillary viscometers and showed quite convincingly that the Newtonian shear viscosity of unimodal suspensions is particle-size independent. Recently, Ackermann & Shen (1979) proposed the following relation which appears to describe very accurately the relative viscosity of monodisperse suspensions:

$$\mu_r = \left(1 - \frac{\pi}{4\alpha^2}\right) + \frac{\pi}{4} \left(1 - \frac{2}{3\alpha}\right) \left(\frac{1}{\alpha^2 - 1}\right) \left(1 + \frac{2}{\sqrt{\alpha^2 - 1}} \tan^{-1} \sqrt{\frac{\alpha + 1}{\alpha - 1}}\right) \quad [22]$$

where  $\alpha = (C_p^\infty / C_p)^{1/3}$  and  $C_p^\infty$  is the maximum attainable solids concentration, presumably equal to the packed-bed volume fraction of solids. When we turn to consider suspensions containing bimodally size-distributed solids, however, we are faced with a tremendous paucity of experimental data and only a single asymptotic theory on which to rely.

Ackermann & Shen (1979) have considered theoretically the viscosity of bidisperse systems in which only very small and very large particles form the solid portion of the mixture. They examined a mixture of total solids concentration  $C$ , of which  $C_{sm}$  and  $C_{la}$  are the concentrations of the small and large particles, respectively. What their analysis amounts to is that the large particles are considered to be in an effective fluid made up of liquid and small particles. This effective fluid has a viscosity, relative to pure liquid, of

$\mu_r(C_{rsm}, C_{sm}^\infty)$  in which  $C_{rsm}$  is the concentration of small particles in the local environment of fluid and small particles only, and is

$$C_{rsm} = C_{sm}/(1 + C_{sm} - C) \quad [23]$$

and  $C_{sm}^\infty$  is the packed-bed volume fraction of small particles. The large particles are then considered to cause the viscosity of the mixture of large particles and pseudo-fluid to increase in exactly the way given by [22]. Thus, the relative viscosity of the total mixture is

$$\mu_{rb} = \mu_r(C_{rsm}, C_{sm}^\infty) \mu_r(C_{la}, C_{la}^\infty). \quad [24]$$

Actually, Ackermann & Shen (1979) considered the shape of both species to be the same so that the maximum attainable concentrations  $C_{sm}^\infty$  and  $C_{la}^\infty$  would be identical. In the present case, such an assumption is unjustified because quite apart from being of different density and size, shape also varied in some of the experiments. The predictions of [24] were compared with the only available data—three measurements by Chong *et al.* (1971) and Sweeney & Geckler (1954) at a diameter ratio of large to small particles of 20.8 and a total solids fraction of 0.55—with remarkable agreement. The only other data available are three further measurements by Chong *et al.* (1971) at particle size ratios of 2.09, 3.19 and 7.24 and the same total solids fraction of 0.55; figure 3 is a plot of the available viscosity data. In view of the fact that  $\mu_{rb}$  at a size ratio of 7.24 differs by only about 10% from the limiting theory, it is probably adequate to represent the data by the dashed lines in the figure. When we come to use the theory to interpret the experimental data later, we will assume that the particle size effect can be handled with sufficient accuracy through a linear interpolation between the monodisperse theory of Ackermann & Shen (1979) [22] and their limiting theory [24] applied at a particle size ratio of four, independent of the total solids concentration. However, rather than taking the quantities  $C_{sm}^\infty$  and  $C_{la}^\infty$  as referring to large and small particles, it seems more realistic to consider the maximum attainable concentration of the mixture itself, particularly when the particles do not differ greatly in size. In view of the uncertainty in estimating the viscosity of bidisperse suspensions of spherical particles, an elaborate procedure is probably unwarranted so we will be satisfied with approximating the mixture's packed-bed solids fraction by a weighted average:

$$C_m^\infty = (C_{la}C_{la}^\infty + C_{sm}C_{sm}^\infty)/(C_{la} + C_{sm}) \quad [25]$$

This allows us to account to some extent for differences in the shape of particles.

At this point we are in a position to complete the balance between viscous and buoyancy forces which will allow us to relate the relative velocity between stream and continuum to measurable and calculable physical properties. For a unit length of stream, the gravity driving force is  $(\pi D^2/4)\Delta\rho_s g$ . For a circular cross-section stream of diameter  $D$  in which viscous forces are confined to a lubricating gap of thickness  $\delta$ , with  $\delta \ll D$ , the viscous force is just  $\mu\mu_{rb}\pi DU_{rel}/\delta$  and a force balance leads immediately to

$$U_{rel} = \frac{\delta D \Delta\rho_s g}{4 \mu \mu_{rb}}. \quad [26]$$

Unfortunately, neither  $\delta$  nor  $D$  can be measured or estimated, although in general the stream diameter is of the order of a few millimeters. As a result, [26] cannot be viewed



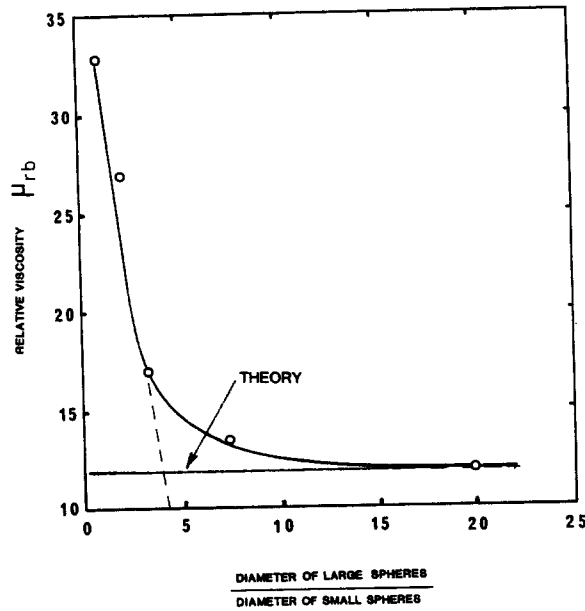


Figure 3. Dependence of the relative viscosity of a bimodally dispersed suspension on the ratio of particle sizes. Data of Chong *et al.* (1971); Theoretical line of Ackerman & Shen (1979). Data are for a total solids concentration of 55% v/v with small spheres occupying 25% of the solids volume.

as predictive; however, a little further analysis is in order. The density difference  $\Delta\rho_s$  is limited by the densities of the packed beds of the two types of particles; therefore, it is useful to scale  $\Delta\rho_s$  on the maximum density difference  $\Delta\rho_s^\infty$ . For later application to experimental measurements, a rearranged form of [26] will be more useful: If we scale  $\Delta\rho_s$  on  $\Delta\rho_s^\infty$ , replace  $\delta$  by  $k'(d_s + d_c)$  and rearrange, we obtain

$$\frac{4U_{rel}\mu_{rb}}{(d_s + d_c)\Delta\rho_s^\infty g} = k'D\frac{\Delta\rho_s}{\Delta\rho_s^\infty}. \quad [27]$$

It will turn out that when *all* experimental data are plotted in the form suggested by [27] (treating  $k'D$  as unknown), a single curve results. Thus, a single fit to all the data will allow prediction of relative velocities, hence, enhanced settling rates, for any other system.

#### EXPERIMENTAL

Experiments were conducted to obtain quantitative data on the effect of system parameters on the rate of settling of model suspensions and on the concentrations of the suspensions produced at either end of the settling vessel following vertical disengagement of the two types of particles from each other. Parameters of primary importance include the concentration, size, density, size distribution and shape of each particle type, fluid density and viscosity, and height and diameter of the settling vessel.

The apparatus consisted of cylindrical tubes having the following dimensions:

Nominal diameter (mm)	Tolerance (mm)	Type
16.4	Laboratory grade	Soda glass
25.4	$\pm 0.005$	Precision bore Pyrex
50.8	Laboratory grade	Pyrex
76.2	$\pm 0.010$	Precision bore Pyrex
	$\pm 0.025$	Precision bore Pyrex

These tubes were aligned vertically on wall-mounting brackets using a theodolite; perfect alignment was sought in order to avoid any convection induced by the presence of inclined surfaces. In many of the experiments one of the two particle types was coated with fluorescent dye to facilitate accurate settling rate measurements. For this purpose, a darkroom was built around the apparatus and observations were made under long-wave ultra-violet illumination.

### *Materials*

Five different fluids were used for the experiments: aqueous thallium formate, carbon tetrachloride, *s*-tetrabromoethane, mixtures of carbon tetrachloride and *s*-tetrabromoethane, and aqueous sucrose solutions. This permitted fluid densities to be varied over the entire range from the buoyant particle density to that of the heavy particles. Fluid viscosity was also varied over the range from 0.0015 to 0.0125 Pa·s.

Two types of polymeric particles were used, polyvinylchloride and polystyrene, as well as a variety of different types of glass ranging in density from 2411 to 3992 kg/m<sup>3</sup>. All solids were screened through new standard sieves, first crudely, and then carefully to obtain single sieve fractions; size fractions ranged from 44–53 μm to 295–354 μm. The plastic powders generally required wet sieving, whereas, glass could be sieved dry. Further details on the fluids used, the properties of the solids and the method of drying the plastic particles can be found in Fessas (1983). In all experiments 0.1% of a surfactant (triton X-100 or Monofax 786, depending on the fluid-particle system) was used to prevent flocculation.

### *Measurements*

Two types of experiments were done: calibration measurements and settling rate experiments. In the former, settling rate vs. concentration data were gathered for each single particle species used. This allowed the later inference of the concentrations of the suspensions collecting at each end of the sedimentation tubes, without actually sampling the suspensions and disturbing the process.

During measurements of the three-phase sedimentation process, the total depth of suspension in the tubes was kept constant. A slug of air at the top of the tube was used to aid mixing of the suspensions. As far as settling rate measurements are concerned, it must be realized that the boundaries between the pure buoyant phase, the mixed region, and the pure heavy phase shown in figure 1 are usually not sharp so it was extremely difficult to follow them with any accuracy. Instead of determining settling rates during the accelerated rate period by following interface positions as a function of time, settling velocities were calculated by measuring the time taken for the heavy and buoyant particles to just separate from each other vertically, and the position of disengagement relative to the ends of the settling tube. This measurement includes the time taken for the streaming flow to be set up, but this was generally very short relative to the total streaming time (only a few per cent of the total time) except for very viscous fluids in short tubes and it introduces negligible error into the measurements. Settling rate measurements on the separated suspensions, on the other hand, were done by following the position of the suspension-fluid interface since this was quite distinct. That operator bias was not a factor in any of the measurements was checked by having three different operators perform six replicate experiments each; the coefficient of variability ranged between 2 and 4%.

## RESULTS AND DISCUSSION

It is appropriate first to compare the theory with the experimental data as a whole, then to examine the influence of each parameter on the enhanced settling rates in turn. There are two separate but related aspects of the model which need to be verified: the verity

of our suppositions about fluid apportioning between streams and continuum, and the utility of [27] as a means of correlating the settling rate data.

### Fluid apportioning

One of the main assumptions made in the theory is that the fluid distributes itself between streams and the surrounding continuum in direct proportion to the volume concentration of the two species and to their packed-bed void fractions. This directly affects the accuracy of prediction of stream and continuum solids concentrations which are themselves deciding factors in determining the density difference  $\Delta\rho$ , driving the convective flow. The most convenient test of these postulates can be had through [10]; this equation suggests that a plot of  $1/C_H^*$  against  $1/C_L^*$  should result in a straight line of slope  $\lambda = \epsilon_H^\infty/\epsilon_L^\infty$  and a  $1/C_H^*$ -intercept of  $(1 - \lambda)$ . Such a plot is shown in figure 4 for the glass/carbon tetrachloride/polyvinylchloride system; the solid line is the model prediction. A large amount of other data has been plotted by Fessas (1983) who always obtained a linear relationship between  $1/C_H^*$  and  $1/C_L^*$ ; however, the model does more than predict a linear relationship—it also suggests what the slope and intercept of the line should be.

Packed bed voidages were measured for 15 sets of experiments similar to the set given in figure 4 and were used to calculate values of  $\lambda$ . These we will call theoretical values. Data sets were also fitted by least-squares straight lines. If the data were perfect and the theory exact, the fitted slope and intercept would result in the same value of  $\lambda$  as was measured from packed bed voidages. The fitted slope and intercept produce experimental values of this parameter which can be compared with the theoretical one. Such a comparison between theory and the measured slope is given in figure 5; the least-squares line passing through the origin in this plot has a slope of  $1.008 \pm 0.056$  with a correlation coefficient of 0.501. (At the 90% confidence level with 15 data points, the correlation coefficient attributable to chance alone is 0.441.) On the other hand, the fitted value of the intercept did not correlate at all with the theoretical value of  $(1 - \lambda)$ . This is not too surprising in view of the fact that  $(1 - \lambda)$  is a small quantity and the scatter in the data themselves is about the same order of magnitude.

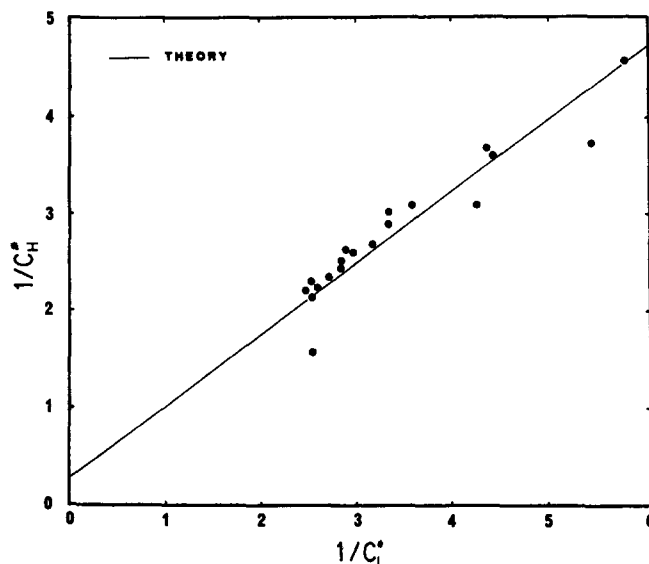


Figure 4. Concentrations of resulting suspensions plotted in the form suggested by [10]. Heavy particles are glass,  $\rho = 2502 \text{ kg/m}^3$ , size = 44–53  $\mu\text{m}$ ; buoyant particles are PVC,  $\rho = 1406 \text{ kg/m}^3$ , size = 90–106  $\mu\text{m}$ ; fluid is carbon tetrachloride,  $\rho = 1586 \text{ kg/m}^3$ ,  $\mu = 0.00152 \text{ Pa}\cdot\text{s}$ ;  $\lambda = 0.753$ .

Our model of fluid apportioning appears to reproduce the data to a good degree of approximation. This especially gratifying since packed bed voidages are only a very rough reflection of particle shape and surface texture. What is more important, however, is the sensitivity of our prediction of stream and continuum suspension densities to errors in  $\lambda$ , i.e. to the nonspherical nature of particles. Calculations indicate that if  $\lambda$  varied from 0.6 to 1.0, the density difference  $\Delta\rho_s$  would vary at most by about 12%. Apparently, the concentrations  $C_H^*$  and  $C_L^*$  are determined largely by those in the initial suspension; roughness effects offer a small correction.

### Settling velocities

All the settling rate data collected (351 measurements) are plotted in figure 6 in the form  $4U_{rel}\mu\mu_{rb}/[(d_H + d_L)\Delta\rho_s^{\circ}g]$  against  $\Delta\rho_s/\Delta\rho_s^{\circ}$  as suggested by [27]. Here,  $d_H$  and  $d_L$  denote the sizes of the heavy and buoyant particles, respectively. Primary parameters were varied over a wide range, including particle densities from 1050 to 3992 kg/m<sup>3</sup>, particles sizes from 44–53  $\mu\text{m}$  to 295–354  $\mu\text{m}$ , volumetric concentrations of the individual species from 2.5 to 45% and total solids concentrations from 5 to 50%.

The striking aspect of figure 6 is that all the data collapse onto a single curve regardless of fluid and particle properties, including particle shape. Evidently the quantity  $k'D$  is not a constant, but *it is a unique function of the buoyancy driving force and is system independent*. In view of the complexity of the three-phase settling phenomenon, this is perhaps a remarkable result. Apart from allowing the prediction of settling rates in virtually any other system, this correlation indicates exactly how each variable in a given system affects the settling rate. Some of these effects are hidden in the various terms and it will be useful to discuss some of them here.

The strength of convection depends on particle size; the larger the particles, the greater will be the relative velocity between streams and counterflowing continuum. But the particle size *ratio* will also have an effect, quite in addition to the sum of the particle sizes. The size ratio  $d_H/d_L$  enters into the estimation of the suspension viscosity within the lubricating layer. Particle densities obviously enter into the density difference ratio

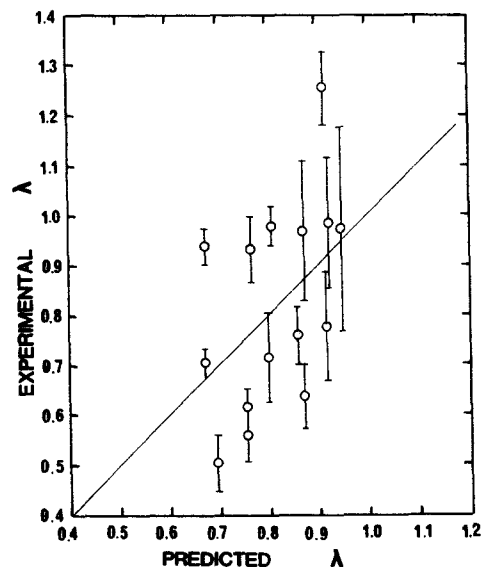


Figure 5. Comparison between measured values of  $\lambda$  and those determined from the slope of lines fitted according to [10]. Error bars represent least-squares standard deviations of the fitted slopes.

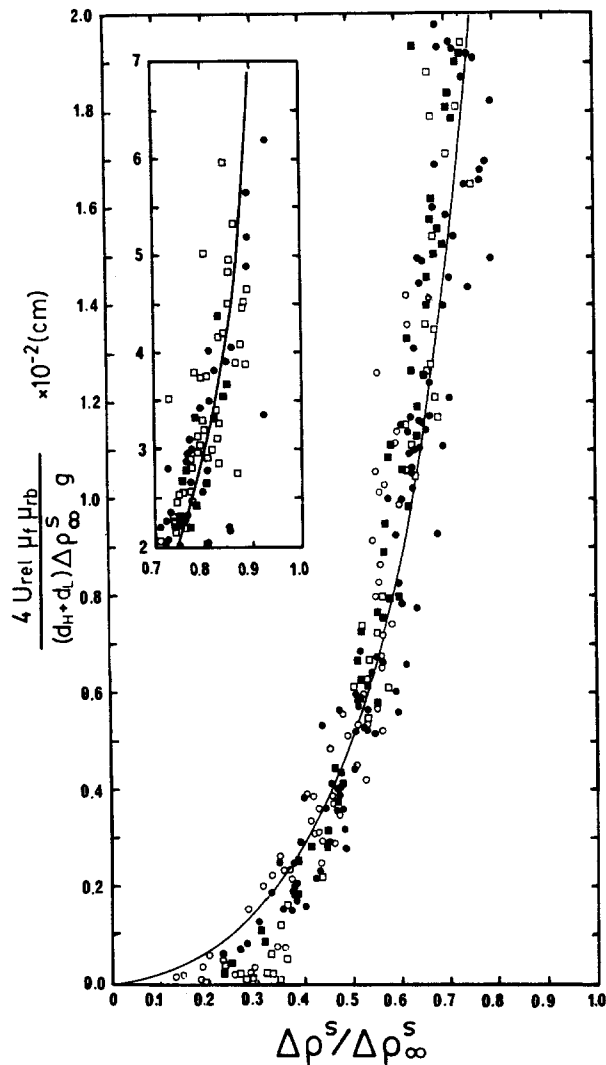


Figure 6. Experimental settling rate data plotted in the form suggested by [27];  $\circ$ , glass/*s*-tetrabromoethane/glass;  $\bullet$ , glass/ carbon tetrachloride/ PVC;  $\square$ , glass/carbon tetrachloride + *s*-tetrabromoethane/glass;  $\blacksquare$ , glass/thallium formate/PVC.

$\Delta \rho_s / \Delta \rho_\infty^S$  but so do the concentrations of the two types of particles in the segregated regions. On the other hand, particle shape enters directly into the calculation of  $\Delta \rho_s^S$  but only indirectly into the viscosity of the suspensions. However, it must be noted that this correlation does not accommodate particle size distribution effects, nor does it seem possible to build these in at the present time.

It is interesting to note that the data in figure 6 seem not to pass through the origin; rather, a finite value of the density difference ratio is needed to produce a relative velocity between streams and continuum. The real explanation is that if the suspensions are too dilute, streams do not form at all; thus there is a minimum concentration and density difference needed to produce convection (note that  $U_{rel}$  is a purely convective velocity and does not include normal hindered settling).

Finally, we point out that the similarity between the lubrication layer in three-phase settling and the plasmatic layer in the flow of suspensions through capillaries is more apparent than real. It is known that for capillary flow the thickness of the plasmatic layer decreases with increasing concentration of the suspension; the opposite is true for sedimentation if one assumes the stream diameter to be concentration independent and

then uses the correlation to estimate the layer thickness. The reason for the opposite sort of behavior is obvious; in capillary flow the shear layer is particle *free*; whereas, in sedimentation the shear layer is a concentrated suspension.

#### *Effect of individual parameters on settling rates*

It is well known that the rate of settling of a single species is greatly affected by suspension concentration. In this work the concentrations of both buoyant and heavy particles were varied and, since our interest is primarily in the improvement to settling rates, results will be reported in terms of the settling and rise velocity ratios  $U_H/U_H^0$  and  $U_L/U_L^0$ . The superscripted quantities refer to the observed velocity of one species in the absence of the other.

In figure 7 is shown the relative increase in the settling velocity of the heavy particles as a function of the volume fraction of the added buoyant phase with the fraction of heavy particles as parameter. Corresponding results for the rise velocity of the buoyant particles are shown in figure 8. The lines in these figures result from a simple generalized correlation of all the data in figure 6. These data were fitted with an equation of the form:

$$\frac{4U_{rel}\mu\mu_{rb}}{(d_H + d_L)\Delta\rho_s^\infty g} = \kappa \left[ \sec\left(\frac{\pi}{2} \frac{\Delta\rho_s}{\Delta\rho_s^\infty}\right) - 1 \right]. \quad [28]^\dagger$$

The least-squares value of the constant  $\kappa$  was found to be 0.130 mm with a standard deviation of  $\pm 0.0021$  mm. The values of this constant was distinguishable among the four sets of data on the figure (taken for different physical systems) only at the 90% confidence level and below.

It is evident from figures 7 and 8 that as the concentration of one species is increased the enhancement to the settling velocity of both itself, and the other species, increases. At a total solids fraction between 0.35 and 0.40 a maximum is reached beyond which further additions of particles causes a diminution in settling rates. The theory correctly predicts the existence of the maximum and the general trend of the data to within the mean error of the generalized correlation (about 30%). A maximum is reached because at about 40% solids the viscosity of the mixture in the lubrication layer increases more rapidly with solids concentration than the buoyancy driving force does.

At very low total solids concentrations the addition of buoyant particles can cause retardation to the settling rate; an example of this is shown in figure 9. Again, the theory predicts this effect although not with good quantitative accuracy. When only a few buoyant particles are added to a dilute suspension of heavy particles, lateral segregation into streams does not usually take place. There appears to be a minimum total concentration of solids needed to produce a sufficiently strong particle-particle interaction to destabilize spatially uniform settling and cause streaming to occur. It is perhaps fortuitous that the model predicts retardation since it is based on a simple fluid mechanical analysis of streaming and none exists at very low concentrations. However, when the curves in figure 9 reached their minimum and begin to turn up, streaming has already set in; this may account to an extent for the success of the theory in this region.

Our simplified theory of convective settling holds the density difference between streams and continuum to be responsible for driving convection. Equation [18] gives this density difference; in terms of initial concentrations in the well-mixed suspension, it is

$$\Delta\rho_s = (\lambda C_H + C_L) \left[ \frac{\Delta\rho_H}{\lambda + C_L(1 - \lambda)} + \frac{\Delta\rho_L}{1 - C_H(1 - \lambda)} \right]. \quad [29]$$

<sup>†</sup>This functional form has no theoretical basis; it merely allows a good fit to most of the data with a single adjustable parameter.

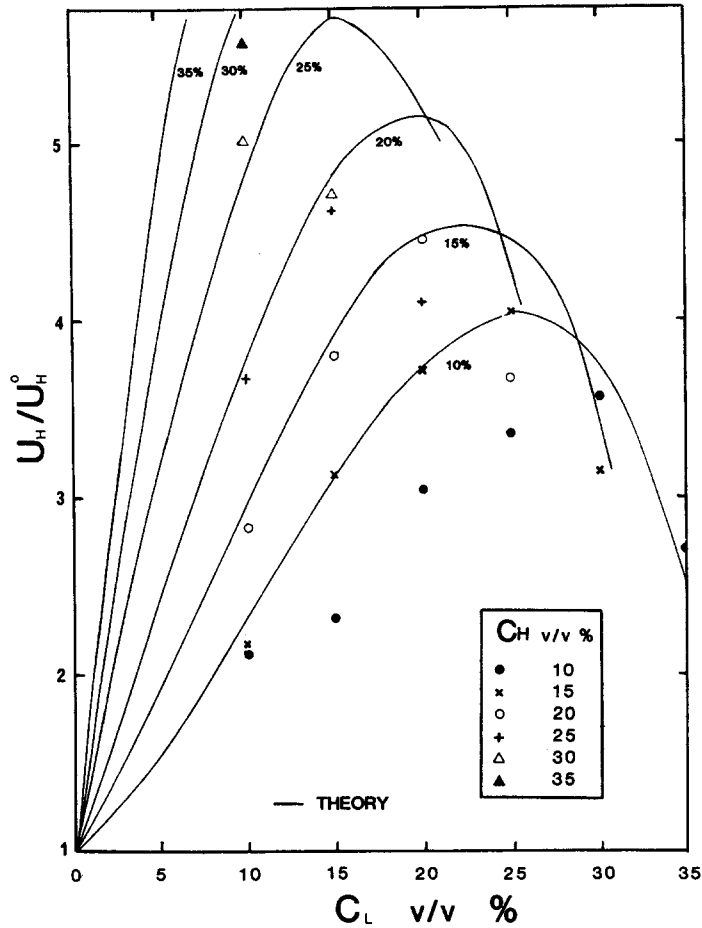


Figure 7. Effect of the concentration of buoyant particles on the normalized settling rate of heavy particles at various initial concentrations of heavy particles. Properties of solids and fluid are the same as in figure 4.

There are two rather interesting features of this equation. First, if the two types of particles have the same packed-bed voidage (i.e. the same shape),  $\lambda = 1$  and [29] reduces to

$$\Delta\rho_s = (C_H + C_L)(\rho_H - \rho_L) \tag{30}$$

and the driving force is independent from the density of the fluid. (Fluid density is contained in  $\Delta\rho_H = (\rho_H - \rho_f)$  and  $\Delta\rho_L = (\rho_f - \rho_L)$  where  $\rho_f$  is the fluid density). Thus, if a convective streaming motion sets up through some instability mechanism, there will be a density difference  $\Delta\rho_s$  driving it even if one of the species is neutrally buoyant or both are heavier than the fluid. On the other hand, if  $\lambda \neq 1$ ,  $\Delta\rho_s$  can either increase or decrease with fluid density depending on whether  $\lambda > 1$  or  $\lambda < 1$ , respectively. We should expect the relative velocities  $U_H/U_H^0$  and  $U_L/U_L^0$  to follow the same pattern since  $U_H$  and  $U_L$  depend directly on  $\Delta\rho_s$ .

One of the reasons why a suspension might be hard to settle is that the density of the suspended particles may not differ much from the fluid density so that the driving force for sedimentation is low. The dependence of the enhanced settling velocity on fluid density is shown in figure 10 for the glass/thallium formate/PVC system in which  $\lambda = 0.673$ ,  $\rho_H = 2960 \text{ kg/m}^3$ ,  $\rho_L = 1400 \text{ kg/m}^3$  and the fluid density was varied from 1458 to 2791  $\text{kg/m}^3$ . Apart from the striking agreement between theory and experiment, perhaps the most interesting observation is that enhancement to the settling rate of heavy particles

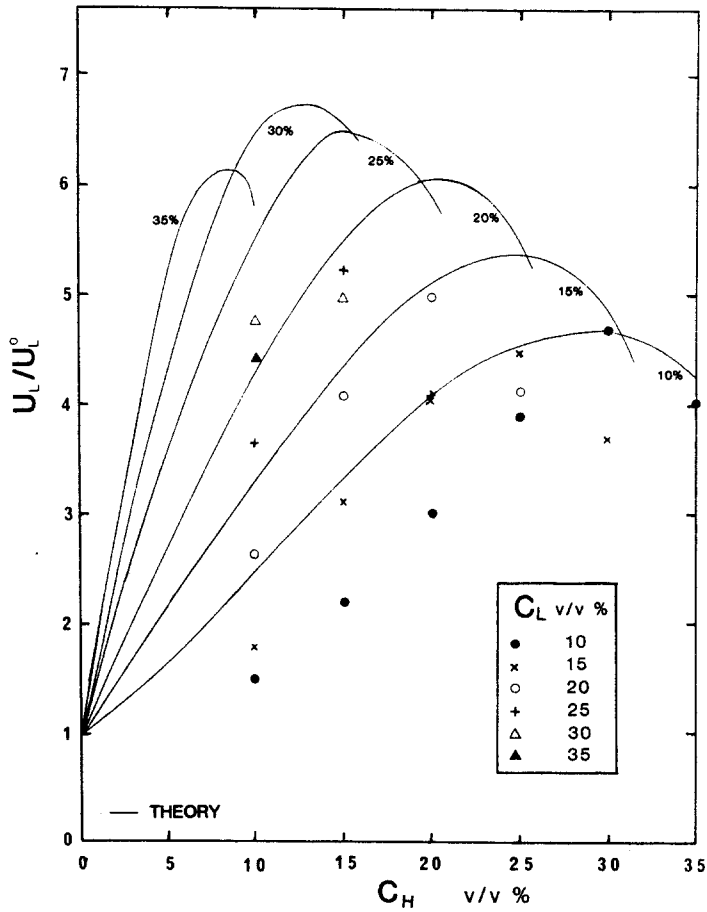


Figure 8. Effect of heavy particle concentration on the normalized rise velocity of buoyant particles with buoyant particle concentration as parameter. Properties of solids and fluid are as in figure 4.

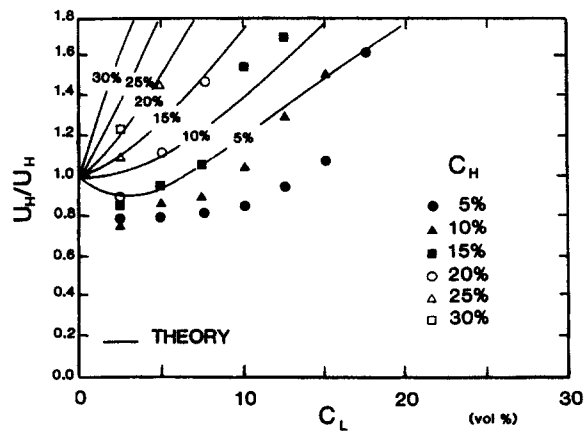


Figure 9. Retardation of the settling rate of heavy particles caused by using low concentrations of buoyant particles. Heavy particles are glass,  $\rho = 2960 \text{ kg/m}^3$ , size = 105–125  $\mu\text{m}$ ; buoyant particles are PVC,  $\rho = 1402 \text{ kg/m}^3$ , size = 105–125  $\mu\text{m}$ ; fluid is thallium formate,  $\rho = 2242 \text{ kg/m}^3$ ,  $\mu = 0.00209 \text{ Pa}\cdot\text{s}$ .



is most pronounced when their density differs least from the fluid. Although it is true that any nonzero  $U_H$  will lead to a large value of  $U_H/U_H^0$  when normalized in this way with  $U_H^0 \rightarrow 0$ , it is also a fact that the enhancement to be realized from buoyant particle addition is enormous. It is noteworthy that even if the two types of particles had the same shape ( $\lambda = 1$ ) so that the relative convective velocity  $U_{rel}$  would be expected not to depend on fluid density,  $U_H/U_H^0$  would still change in the fashion of figure 10 because as the fluid and heavy-particle densities approached each other,  $U_H^0$  would tend to zero and the ratio  $U_H/U_H^0$  would increase rapidly.

The effect of changing the density of the heavy particles was what one would expect from figure 10; the closer they were to the fluid density, the greater was the enhancement to the settling velocity from adding buoyant particles. By analogy, one might expect that the enhancement will be greater, the lower is the density of the buoyant particles. To an extent this is true; however, if they are too buoyant (or too big) they tend to carry some of the heavy phase to the top of the vessel with them (Vilambi 1982). This results in a less clean cut separation.

Buoyant and heavy particle sizes were varied individually in two separate sets of experiments. The results, presented in figures 11 and 12, show that as the size of the buoyant particles is increased the settling of the heavy particles becomes more pronounced, and vice versa. Thus, the presence of large particles of one type generally accelerates the settling of small particles of the other type; there is a practical limit, of course, because if particles that are too large are used they tend to entrain large amounts of small particles of the opposite species with them.

On the other hand, increases in the size of one type of particles affect the settling rate of that same species in a strongly negative way. An example is shown in figure 13 in which the degree of enhancement to the settling rate of heavy particles is plotted as a function of their own size. This decreased effectiveness is a result of the fact that when *small* buoyant particles are added to large settling ones, they increase the thickness of the lubrication layer but little while at the same time increasing the viscosity of the mixture in the gap a great

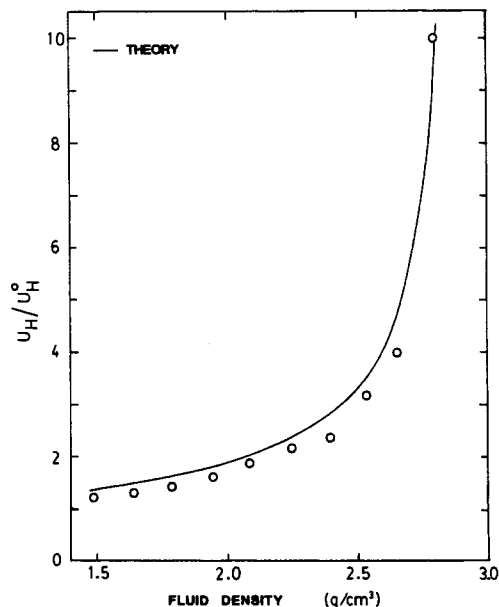


Figure 10. Dependence of the normalized settling velocity of heavy particles on the fluid density for initial concentrations of heavy and buoyant particles of 12.5 and 15%, respectively. Particles are the same as in figure 9. Viscosity of aqueous thallium formate ranged from 0.00128 to 0.00335 Pa-s when the density was varied from 1500 to 2800 kg/m<sup>3</sup>.

deal. Indeed, if very small buoyant particles are added to a suspension of very large ones in sufficient quantity, settling rates can become retarded below the single species values. The theory accounts at least qualitatively for all of these effects, and to a large measure the agreement is quantitative.

The dependence on particle size is very strong with the greatest degree of improvement being had with the addition of the largest possible buoyant particles consistent with a clean separation of the two species. Finally, it is of some practical importance to note that the

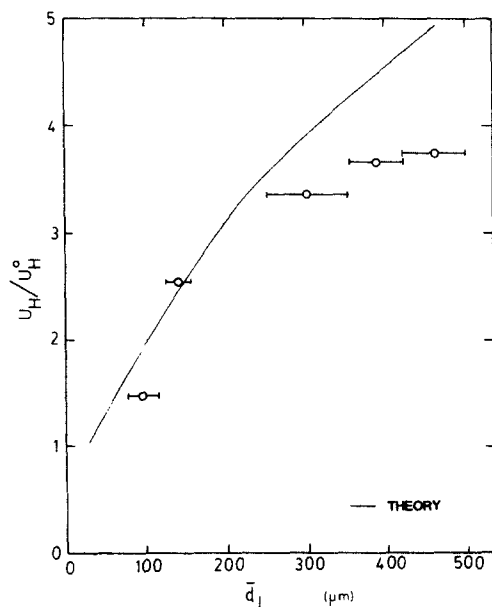


Figure 11. Effect of the size of buoyant particles on the settling velocity of the heavy phase; both solids at 15% initial concentration. Heavy particles are PVC,  $\rho = 1400 \text{ kg/m}^3$ , size = 105–125  $\mu\text{m}$ ; buoyant phase is polystyrene,  $\rho = 1040 \text{ kg/m}^3$ , bars indicate sieve size range; fluid is aqueous sucrose,  $\rho = 1107 \text{ kg/m}^3$ ,  $\mu = 0.00224 \text{ Pa}\cdot\text{s}$ .

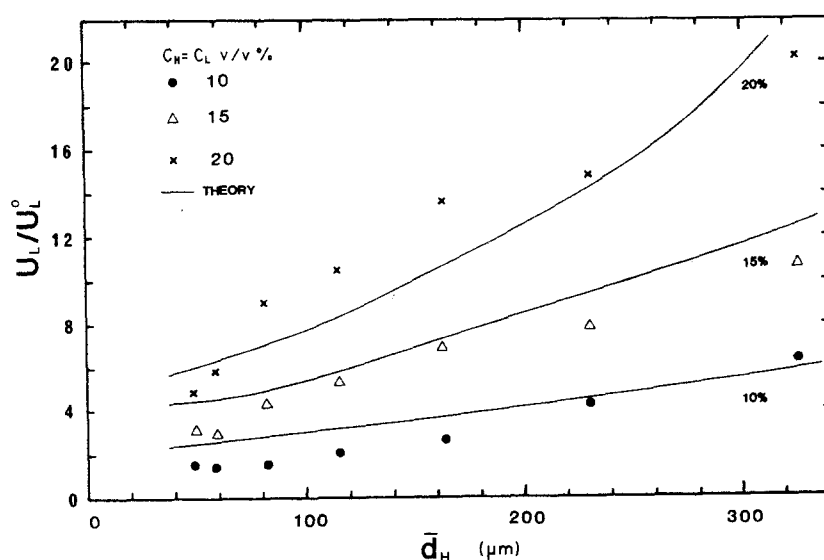


Figure 12. Variation of buoyant particle rise velocity with size of the heavy particles. System is glass ( $\rho = 2475 \text{ kg/m}^3$ )/carbon tetrachloride ( $\rho = 1586 \text{ kg/m}^3$ ,  $\mu = 0.00152 \text{ Pa}\cdot\text{s}$ )/PVC ( $\rho = 1406 \text{ kg/m}^3$ , size = 90–106  $\mu\text{m}$ ).

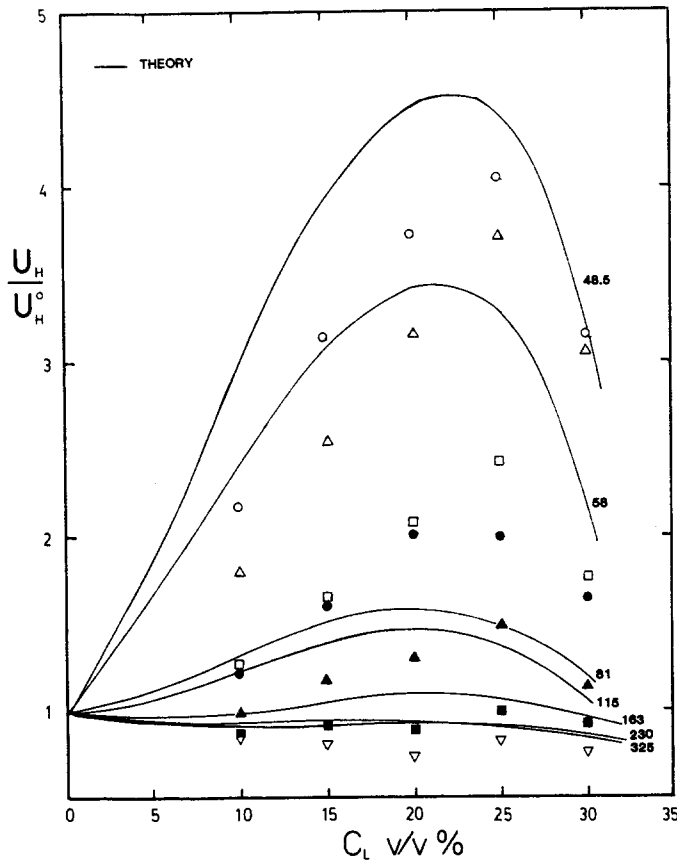


Figure 13. The degree of enhancement to the settling rate of heavy particles as a function of their own size. System and properties as in figure 12.

smallest particles are the ones whose settling rates are most improved by the addition of particles of the opposite effective density; these are the very ones that are most difficult to settle in the first place.

In the settling of natural slurries, the spread of the particles size distribution is an important parameter affecting the sedimentation rate of one-particle-density suspensions. In the sedimentation of not-too-concentrated polydisperse slurries there is a gradual vertical segregation of the suspension according to particle size which leads to gradually varying line settling rates. However, Scott & Mandersloot (1979) have found for sufficiently concentrated suspensions that settling takes place uniformly at a velocity calculable using the Stokes mean diameter  $d_o$ , of the polydisperse mixture:

$$d_o = (d_v^3 d_l / d_s^2)^{1/2} \tag{31}$$

in which  $d_l$ ,  $d_s$  and  $d_v$  are the lineal, surface and volume mean sizes, respectively. For log-normal distributions, these are related to the geometric mean (50% median) size,  $d_g$  and the geometric standard deviation,  $\sigma_g$ , by an equation of the form  $\ln d = \ln d_g + \alpha (\ln \sigma_g)^2$  (Allen 1981) where the sizes  $d_l$ ,  $d_s$  and  $d_v$  have corresponding values of  $\alpha$  of 0.5, 1.0 and 1.5. Thus, the Stokes diameter can be expressed in terms of  $d_g$  and  $\sigma_g$  by the following relation:

$$\ln d_o = \ln d_g + 1.5 (\ln \sigma_g)^2. \tag{32}$$

Experiments were conducted in which the spread in the size distribution of one type of particles was varied while the other type of particles was kept monodisperse. Size distributions were log normal and were made up synthetically from closely sieved fractions. Having chosen  $\sigma_g$ , we made up mixtures around a median size,  $d_g$ , so that the Stokes diameter given by [32] remained constant. The results of experiments in which the heavy particles were size distribution are shown in figure 14 and we note in passing that for  $\sigma_g$  in the range 1.05–1.25 no variation in the settling velocity of the heavy particles alone was found. The theoretical lines in figure 14 are based on the Stokes diameter; of course, the theory is not capable of accounting for particle size distribution effects so none are shown. The most interesting result is that the enhancement to settling rates is totally unaffected by fairly wide particle size distributions. Evidently, the addition of buoyant particles is no less effective with polydisperse suspensions than it is with monodisperse ones. In a practical sense this is an important finding.

The remaining system parameter to be discussed is the fluid viscosity. The results of experiments using three different viscosities are shown in figure 15 in a form suggested by the theory. The observed inverse dependence of velocity on fluid viscosity is consistent with the assumption of the theory that the lubrication layer contains a laminar flow. This parameter will be found to have a more interesting effect, however, when we come to consider the effects of tube or vessel geometry.

All of the data reported so far were taken in settling tubes of 25.4 mm i.d. This is nearly 80 times larger than the mean size of the largest particles used (295–354  $\mu\text{m}$ ). However, the streams are of the order of 3 mm wide, an appreciable fraction of the tube diameter, so that tube size might affect the settling process. That it does not is shown by the data of figure 16. This suggests that the segregation of the two species is a purely local effect; particles probably do not translate laterally over distances much greater than the width of the streams that eventually evolve. The buoyant phase used in these experiments was not sieved, nor was the standard deviation of its size distribution measured; the theoretical lines in this figure are based on the median diameter of 125  $\mu\text{m}$ .

The effect of the length of the settling tube on sedimentation velocities has been reported elsewhere (Fessas & Weiland 1982) where it was noted that if the tubes were too short, the streaming motion did not have sufficient time to be set up. Tube length effects were also found to be more pronounced for high viscosity fluids. However, all the data

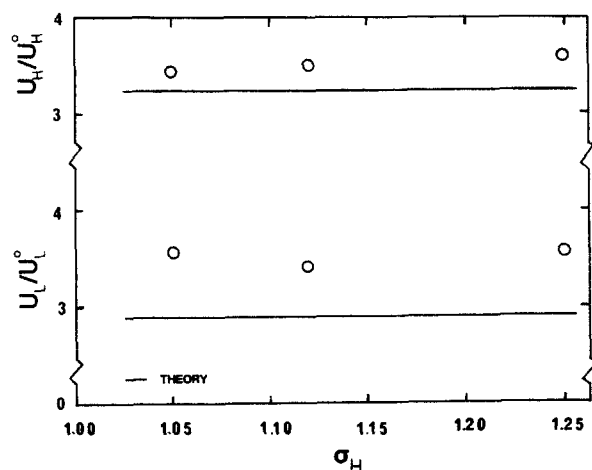


Figure 14. The effect of spread in size distribution of the heavy particles on normalized settling and rise velocities. Mean Stokes diameter of all particles is 114.4  $\mu\text{m}$ ; heavy phase is glass ( $\rho = 2475 \text{ kg/m}^3$ ); buoyant phase is PVC ( $\rho = 1404 \text{ kg/m}^3$ ); fluid is carbon tetrachloride ( $\rho = 1586 \text{ kg/m}^3$ ,  $\mu = 0.00152 \text{ Pa}\cdot\text{s}$ ).

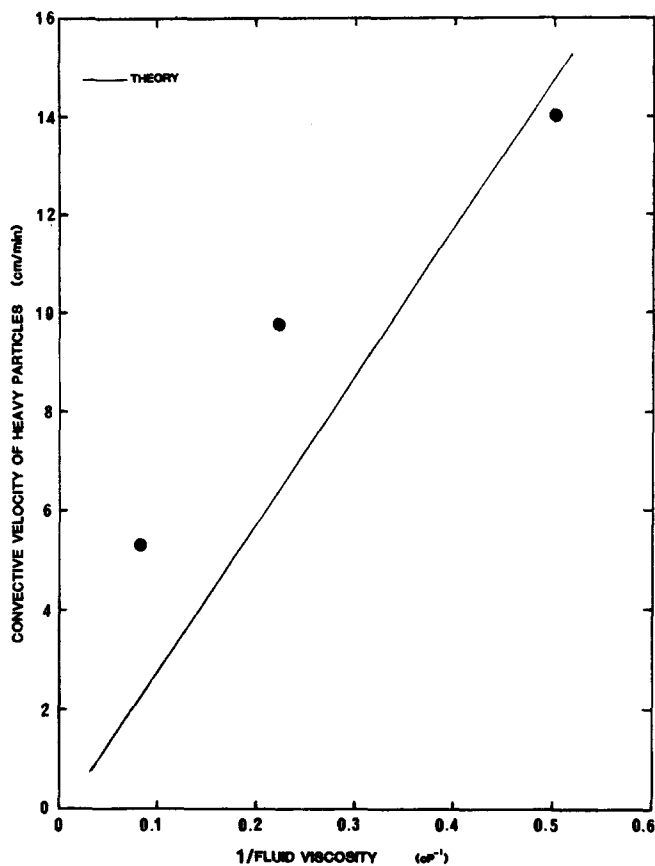


Figure 15. Convective settling velocity of the heavy phase as a function of fluid viscosity. Both types of particles have the properties of those in figure 9. Fluids were aqueous thallium formate and glycerol having  $\rho = 2300 \text{ kg/m}^3$ .

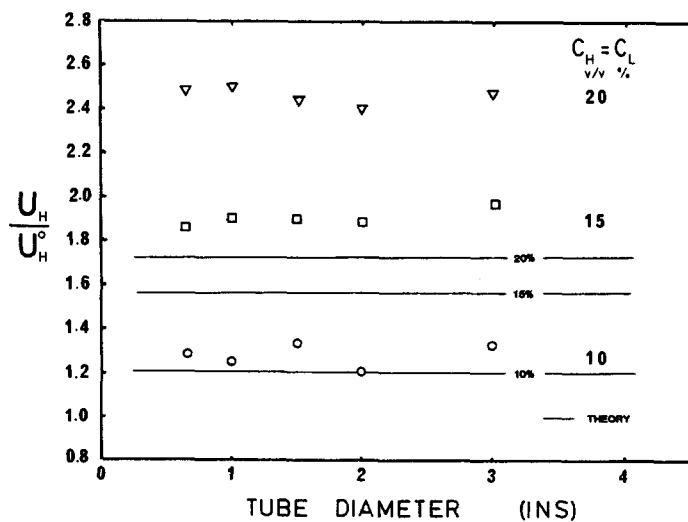


Figure 16. Experimental data indicating that enhanced settling rates are independent of vessel diameter. System is glass ( $\rho = 2491 \text{ kg/m}^3$ , size =  $105\text{--}125 \mu$ )/carbon tetrachloride ( $\rho = 1586 \text{ kg/m}^3$ ,  $\mu = 0.00152 \text{ Pa}\cdot\text{s}$ )/PVC ( $\rho = 1406 \text{ kg/m}^3$ , unsieved).

presented in the present communication were obtained using tubes of great enough length (540 mm) for this effect to be negligible.

From a practical viewpoint, perhaps the most important conclusion that can be drawn from this study is that buoyant particle addition is most effective in accelerating the settling rates of the most difficult to sediment suspensions. Enhancement is greatest with *small* particles of density only *slightly* more than the fluid, settling in *high* viscosity liquids. Furthermore, the effect is most pronounced with large buoyant particles rather than small ones. In any practical application, the buoyant particles would undoubtedly have to be recycled; large particles are relatively easier to separate from the fluid than the small ones. Finally, the fact that the spread of particle size distributions seems not to affect the efficacy of the three-phase-settling process has positive practical implications. All of these considerations suggest that buoyant particle addition is a promising means for accelerating sedimentation rates of difficult-to-separate suspensions.

The simple theory of the steady streaming process presented here seems adequately to reflect the experimental findings. Perhaps its greatest weakness lies in the tremendous lack of information about the viscosity of bimodally dispersed suspensions. Nevertheless, theory and experiment are in good accord. On the other hand, the theory does not address the cause of the lateral segregation at all; as a result, we are left quite uncertain about whether streaming will even occur in any given situation. This appears to be a question of hydrodynamic stability, certainly a fascinating area for future research.

*Acknowledgements*—This work was supported by grants from the Australian Research Grants Committee (Grant No. F79/15186 I), the National Science Foundation (Grant No. CPE-8023185) and the United States Environmental Protection Agency (Grant No. R808519-01). YPF was initially supported by University of Queensland Graduate Fellowship. The generosity of the Diamond Shamrock Corp., B. F. Goodrich (Australia) Ltd. and Mona Industries, Inc. in donating materials is gratefully acknowledged.

#### REFERENCES

- ACKERMANN, N. L. & SHEN, H. T. 1979 Rheological characteristics of solid-liquid mixtures. *AIChE J.* **25**, 327-332.
- ALLEN, T. 1981 *Particle Size Measurement*, 3rd Edn. Chapman & Hall, London.
- BHATTY, J. I., DAVIES, L., DOLLIMORE, D. & GAMLEN, G. A. 1980 Particle-cluster formation and associated liquid in the sedimentation of Ballotini in aqueous glycerol. *Powder Technol.* **25**, 53-56.
- BRADLEY, W. H. 1965 Vertical density currents. *Science* **150**, 1423-1428.
- CHESTERS, A. K., VAN DOORN, M. & GOOSENS, L. H. J. 1980 A general model for unconfined bubble plumes from extended sources. *Int. J. multiphase Flow* **6**, 499-521.
- CHONG, J. S., CHRISTIANSEN, E. B. & BAER, A. D. 1971 Rheology of concentrated suspensions. *J. Appl. Polymer Sci.* **15**, 2007-2021.
- CRABTREE, J. R. & BRIDGEWATER, J. 1969 Chain bubbling in viscous liquids. *Chem. Engng Sci.* **24**, 1755-1768.
- FESSAS, Y. P. 1983 On the settling of model suspensions promoted by rigid buoyant particles. Ph.D. Thesis, Clarkson College of Technology, Potsdam, New York.
- FESSAS, Y. P. & WEILAND, R. H. 1981 Convective solids settling induced by a buoyant phase. *AIChE J.* **27**, 588-592.
- FESSAS, Y. P. & WEILAND, R. H. 1982 convective solids settling induced by a buoyant phase—a new method for the acceleration of thickening. *Resources and Conservation* **9**, 87-93.

- HAPPELL, J. 1958 Viscous flow in multiparticle systems: slow motion of fluid relative to beds of spherical particles. *AIChE J.* **4**, 197-201.
- HUSSAIN, N. A. & SIEGEL, R. 1976 Liquid jet pumped by rising gas bubbles. *J. Fluids Engng, Trans ASME Ser. I* **98**, 49-57.
- KARNIS, A., GOLDSMITH, H. L. & MASON, S. G. 1966 The flow of suspensions through tubes. *Can. J. Chem. Engng* **44**, 181-193.
- MAUDE, A. D. & WHITMORE, R. L. 1956 The wall effect and viscometry of suspensions. *Brit. J. Appl. Phys.* **7**, 98-102.
- RIETEMA, K. & OTTENGRAF, S. P. P. 1970 Laminar liquid circulation and bubble street formation in a gas-liquid system. *Trans. Inst. Chem. Engrs* **48**, 54-62.
- SCOTT, K. J. & MANDERSLOOT, W. G. B. 1979 The mean particle size in the hindered settling of multisized particles. *Powder Technol.* **24**, 99-101.
- SMITH, T. N. 1965 The differential sedimentation of particles of two different species. *Trans. Inst. Chem. Engrs* **43**, 69-73.
- SWEENEY, U. H. & GECKLER, R. D. 1954 The rheology of suspensions *J. Appl. Phys.* **25**, 1135-1114.
- VILAMBI, N. R. K. 1982 Enhanced settling of industrial suspensions using positively buoyant particles. M. S. Thesis, Clarkson College of Technology, Potsdam, New York.
- WEILAND, R. H. & MCPHERSON, R. R. 1979 Accelerated settling by addition of buoyant particles. *Ind. Engng Chem. Fundls.* **18**, 45-49.